Bone Reports 8 (2018) 1–8

Contents lists available at ScienceDirect

Bone Reports

journal homepage: www.elsevier.com/locate/bonr

Decisive differences in the bone repair processes of the metaphysis and diaphysis in young mice

Satoshi Inoue, Hirotada Otsuka, Jiro Takito, Masanori Nakamura*

Department of Oral Anatomy and Developmental Biology, Showa University School of Dentistry, 1-5-8 Hatanodai, Shinagawa-ku, Tokyo 142-8555, Japan

ARTICLE INFO

Keywords:
Bone healing
Metaphysis
Diaphysis
Bone marrow
Periosteum

ABSTRACT

Fractures are common traumatic injuries that mainly occur in the metaphyses of long bones such as the proximal humerus, distal radius, and proximal femur. However, most studies of fracture repair processes have focused on the diaphyseal region. In this study, we compared the bone repair processes of the metaphysis and the diaphysis of the mouse tibia. Bone apertures were formed in the tibial metaphysis and diaphysis. At indicated times after surgery, samples were collected, and the healing process was investigated using micro-computed tomography, as well as histological, immunohistochemical, and mRNA expression analyses. In the metaphysis, cartilage formation was not detected on the periosteal side. The bone aperture was filled with newly formed bone produced from bone marrow at day 7. In the case of the diaphysis, cartilage was formed around the aperture at day 4 and sequentially replaced by bone on the periosteal side. The bone aperture was filled with newly formed bone at day 14. In the bone marrow, expression of the osteogenic markers such as alkaline phosphatase, osteocalcin, and type I collagen, appeared earlier with metaphyseal injury than with diaphyseal injury. The mRNA expression of chondrogenesis markers was markedly upregulated in the diaphysis compared with that in the metaphysis on the periosteal side. These results indicate differences in the bone repair processes of the two regions, suggesting functional heterogeneity of the periosteum and bone marrow mesenchymal cells in response to bone fractures.

1. Introduction

Long bones are anatomically divided into a cancellous bone-rich metaphysis at each end and the cortical-rich diaphysis in the center (Standring, 2015). In humans, fractures are common traumatic injuries that mainly occur in the metaphyseal regions of long bones such as the proximal humerus, distal radius, and proximal femur (Hedström et al., 2010; Driessen et al., 2016). However, most studies of the bone repair process have focused on the diaphyseal region, in which bone repair has been widely studied (Schindeler et al., 2008; Einhorn and Gerstenfeld, 2015). Experimental models for bone repair in the diaphysis have involved various animals, methods, and ages (Histing et al., 2011; Mills and Simpson, 2012). In the diaphysis, the bone repair process is divided into four histological stages on the periosteum side: inflammation, soft (cartilaginous) callus formation, hard (bony) callus formation, and remodeling (Schindeler et al., 2008; Einhorn and Gerstenfeld, 2015). The initial stage after injury is characterized by hematoma formation and subsequent inflammation. After inflammation, a cartilaginous callus is formed around the fracture site and then is gradually replaced by a bony callus. The bony callus is remodeled to the original bone architecture by osteoclasts. The presence of the bony callus is one of the important criteria for assessment of fracture union (Corrales et al., 2008). As a commonly used model for closed fractures, an intramedullary pin is inserted into the medullary canal of a long bone, and then the bone is bent or cut to produce a stable fracture (Bonnarens and Einhorn, 1984); thus, in this fracture model the medullary callus has been ignored.

In contrast, it has been suggested that stable metaphysis fractures are repaired by direct bone formation within the bone marrow and that cartilaginous and bony callus formation are not observed on the periosteum side (Jarry and Uhthoff, 1971; Uhthoff and Uhthoff and Rahn, 1981; Chen et al., 2015; Han et al., 2015). The histological stages of the metaphyseal repair process are also different from those of the diaphyseal repair process (Chen et al., 2015; Han et al., 2015). Han (Han et al., 2015) reported that the metaphyseal repair process is divided into five histological stages in the bone marrow. The first stage is characterized by a bleeding event, and inflammation is reduced compared to that observed in the diaphysis. The second stage is mesenchymal stem cell activation and differentiation into osteoblasts, and the third stage is the formation of woven bone. The fourth stage is characterized by the transformation of the newly formed woven bone to lamellar bone, followed by a shift to the final stage of continuous bone

* Corresponding author.
E-mail address: masanaka@dent.showa-u.ac.jp (M. Nakamura).

https://doi.org/10.1016/j.bonr.2017.11.003
Received 4 March 2017; Received in revised form 17 October 2017; Accepted 23 November 2017
Available online 24 November 2017

remodeling. In humans, the repair process of the metaphysis also lacks cartilage formation, and direct bone formation has been observed in bone marrow by biopsies of distal radius fractures (Aspenberg and Sandberg, 2012). In the repair processes of the two sites, the effects of several drugs are also different (Sandberg and Aspenberg, 2015a; Sandberg and Aspenberg, 2015b; Sandberg et al., 2016). Non-steroidal anti-inflammatory drugs (NSAIDs) and glucocorticoids inhibit diaphysis healing but not metaphysis healing (Sandberg and Aspenberg, 2015a; Sandberg and Aspenberg, 2015b). Furthermore, alendronate, a bisphosphonate that inhibits osteoclastic bone resorption, increases the amount of medullary callus earlier in the metaphysis than in the diaphysis (Sandberg et al., 2016). These results indicate clear differences in the repair processes and effects of drugs between the two sites.

Mesenchymal stem cells residing close to the bone surface exhibit different activities (Siclari et al., 2014; Guarnerio et al., 2014) and stronger osteogenic potential than those in the central bone marrow (Siclari et al., 2014). The cancellous bone-rich metaphyseal region has more mesenchymal progenitors than the diaphyseal region. Generally, bone repair in the cancellous bone-rich metaphysis is considered to progress faster than that in cortical bone-rich sites such as the diaphysis (Brown et al., 2014), but there is no clear evidence of time-specific kinetic differences in bone repair between these two regions.

In terms of bone repair processes, it is important for fracture management to have a clear understanding of the time course of the appearance of callus and the cells related to bone repair. However, there have not yet been any reports that have chronologically analyzed callus formation and bone repair-related cell differentiation directly in both regions of bone. Fracture in long bone healing in humans is quite similar, but not completely identical to that described for laboratory animals (Postacchini et al., 1995). In this study, we used adolescent mice as experimental animals, and compared the repair processes under mechanically stabilized conditions of the metaphysis and diaphysis of tibia.

2. Materials and methods

2.1. Animals

Male ICR mice (8 weeks old) were obtained from Sankyo Laboratories (Tokyo, Japan) and maintained under specific pathogen-free conditions.

2.2. Bone injury model

A total of 78 mice were divided into two groups: the metaphysis injury group (39 mice) and the diaphysis injury group (39 mice). Mice from each group were anesthetized using 2% inhalational isoflurane before surgery. The skin of the right hind limb overlaying the tibia was shaved, and then the skin, muscle, and periosteum were incised along the medial part of the tibia. A bone aperture was formed from medial through both sides cortical bone in the metaphysis or diaphysis, respectively, using a round bur (diameter 0.8 mm; AS ONE, Osaka, Japan). Bone apertures were unilateral in each mouse, and the metaphysis and diaphysis were located about 1.5 mm and 6 mm from the growth plate, respectively (Fig. 1A). The skin was sutured at the end of surgery. This model was stable without external fixation (He et al., 2011). There was no additional injury around the bone aperture during the healing period, and mice exhibited the normal walking activity.

The injured right tibiae were collected day 3, 4, 5, 7, 14, 21, 28, 35, and 42 after surgery (n of 6 at day 3, 4, 5, 7; n of 3 at day14, 21, 28, 35, 42).

2.3. Micro-computed tomography (micro-CT)

Tissue samples were fixed in 4% paraformaldehyde (PFA) in phosphate-buffered saline (PBS). Newly formed bone was imaged ex vivo using the ScanXmate-L090H (Comscan Techno, Kanagawa, Japan). Imaging conditions were as follows: 87 kV, 37 μA, voxel resolution 14 μm per voxel, and 992 × 992 pixel image matrices. Three-dimensional imaging data were reconstructed by conneCT express software (White rabbit, Tokyo, Japan). Newly formed bone and bone mineral density (BMD) were analyzed using TRI-3D BONE (Ratoc CO, Tokyo, Japan). BMD calibration was performed using phantom materials with known bone mineral densities. Regions/measurements of interest included the periosteal region (periosteal callus, bone volume (BV), mm^3), bone marrow [medullary callus, bone volume/tissue volume (BV/TV), %], and bone defect area (BMD, mg/cm^3), as shown Fig. 1B.

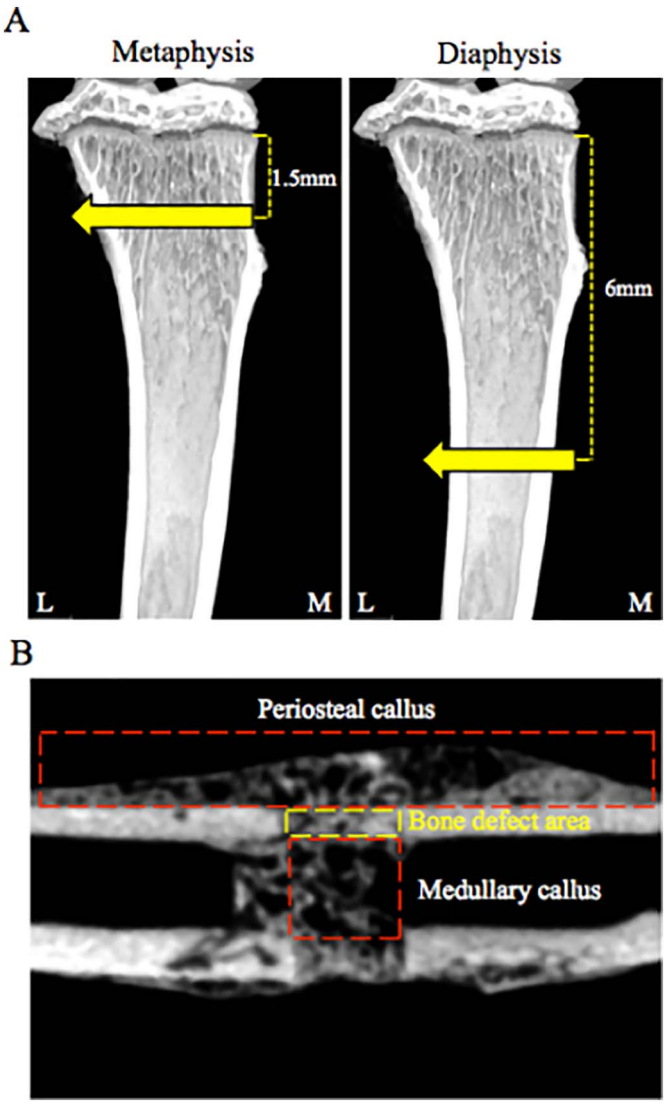

Fig. 1. Schematic diagram of the bone injury site and region of interest (ROI).
A. Bone aperture in the metaphysis and diaphysis were located about 1.5 mm, 6 mm from growth plate, respectively.
B. ROI for analysis periosteal callus, medullary callus, and BMD.

2.4. Histological and immunohistochemical analyses

After analyzed by micro-CT, samples were decalcified with 10% EDTA; some samples were dehydrated in a graded series of ethanol followed by xylene and then embedded in paraffin. To confirm cartilage formation, sections (5 μm in thickness) were stained with toluidine blue at pH 4.1, or with safranin O/fast green, respectively. Toluidine blue-stained images were taken at × 4 magnification using a microscope (Bz-700-All-in-one; KEYENCE, Osaka, Japan), and metachromatic areas

were measured.

Other samples were immersed in 5%, 15%, and then 30% sucrose, embedded in Tissue Tek O.C.T. compound (Sakura Finetek Japan, Tokyo, Japan), and quickly frozen in a mixture of acetone and dry ice. Frozen sections (7 μm in thickness) were cut and placed on SILANE-coated glass slides and air dried. Alkaline phosphatase (ALP) activity was determined using alkaline phosphatase substrate III (Vector Laboratories, Burlingame, CA, USA) to observe osteogenic cells.

To detect type I collagen, sections were digested with testicular hyaluronidase (25 mg/ml in PBS; Sigma Chemical, St. Louis, MO, USA) for 1 h at 37 °C. After rinsing with PBS, each section was incubated with 5% normal goat serum in PBS containing 5% bovine serum albumin and 0.025% Triton X-100 for 1 h and then incubated with rabbit anti-mouse type I collagen antibody (1:1000-diluted, Rockland, Limerick, PA, USA) or rabbit anti-mouse osteocalcin antibody (1:100-diluted, Abcam, Cambridge, UK). After rinsing with PBS, the sections were incubated with Texas red-labeled goat anti-rabbit IgG secondary antibody (Vector Laboratories). After rinsing with PBS, sections were observed under the fluorescence microscope (Bz-700-All-in-one; KEYENCE). The region of interest on the periosteum side was the lateral side of the tibia.

2.5. Quantitative real-time PCR (qPCR)

The periosteum and bone marrow were dissected from each injured tibia under a microscope and immersed in RNAlater (Sigma-Aldrich Japan, Tokyo, Japan). Total RNA was extracted from each sample using an RNeasy Universal kit (Qiagen, Tokyo, Japan). PrimeScript II 1st strand cDNA Synthesis Kit (Takara Bio, Shiga, Japan) was used for RT-PCR to synthesize cDNA. THUNDERBIRD SYBR qPCR Mix (TOYOBO, Osaka, Japan) and a Lightcycler 96 (Roche, Basel, Switzerland) were used for all real-time PCR amplifications. A two-step amplification (15 s at 95 °C, 60 s at 60 °C) was run for 55 cycles after an initial 10 min denaturation. β-actin mRNA levels were quantified as an internal control, and relative expression ratios were calculated using the ΔΔCt method. The primer sequences used for PCR are listed in Table 1.

2.6. Statistical analysis

Differences between groups were evaluated using unpaired Student's *t*-tests. P values < 0.05 were considered statistically significant (n of 3 for each time point).

2.7. Ethical approvals

Approval for this study was obtained from the ethics committee of the Showa University School of Dentistry (approval number: 16017).

Table 1
Used primer pairs.

Name	Primer sequence	Size
β-actin	Forward: 5′-AGCCATGTACGTAGCCATCC-3′ Reverse: 5′-GCTGTGGTGGTGAAGCTGTA-3′	222 bp
Sox9	Forward: 5′-AGGAAGCTGGCAGACCAGTA-3′ Reverse: 5′-CGTTCTTCACCGACTTCCTC-3′	193 bp
Type2 collagen2a1	Forward: 5′-GGGCTCCCAGAACATCACCTACCA-3′ Reverse: 5′-TCGGCCCTCATCTCCACATCATTG-3′	120 bp
Osterix	Forward: 5′-AGGCACAAAGAAGCCATAC-3′ Reverse: 5′-AATGAGTGAGGGAAGGGT-3′	162 bp
Runx2	Forward: 5′-GAGAGGTACCAGATGGGACT-3′ Reverse: 5′-CACTTGGGGAGGATTTGTGA-3′	194 bp
Type1 collagen1a1	Forward: 5′-CCTGGAATGAAGGGACACCG-3′ Reverse: 5′-CCATCGTTACCGCGAGCACC-3′	194 bp

3. Results

3.1. Cartilage formation on the periosteal side

To analyze cartilage formation, sections were stained with toluidine blue or safranin O/fast green. In the metaphysis, the periosteum thickened slightly from day 3 to day 5 (Fig. 2A, B). However, while a small amount of safranin O stain was detected near the metaphysis healing site, it was located to sites of calcified cartilage from the epiphyseal plate and was not cartilage tissue associated with the healing callus tissue (Fig. 2A–C). In contrast, cartilage formed around the bone aperture in the diaphysis by day 4–7, as evidenced by metachromatic staining, and safranin O (Fig. 2A, B). Cartilage formation peaked at day 5, and the cartilage eventually disappeared by day 14. There were significant differences in the areas between the metaphysis and the diaphysis at days 5 and 7 (Fig. 2C).

3.2. Micro-CT analysis

3.2.1. Periosteal callus

To confirm bony callus formation, we assessed the periosteum and bone marrow using micro-CT. In the metaphysis, a small amount of bone formation was observed at days 5 and 7 (Fig. 3A, B). In contrast, newly formed bone was detected around the bone aperture in the diaphysis at day 7 (Fig. 3A). Periosteal callus (BV) peaked at day 14 and bridged the bone aperture (Fig. 3A, B). Subsequently, the periosteal callus fused to the cortical bone and was remodeled. A significant difference was found in periosteal callus (BV) from day 7 to 28 between the two bone regions (Fig. 3B).

3.2.2. Medullary callus

The medullary callus formed earlier in the metaphysis than in the diaphysis, at day 5 (Fig. 3A, C). Medullary callus formation(BV/TV) peaked at day 7 and gradually decreased from day 14 to day 42. The bone aperture was filled with medullary callus at day 7 and then fused to the cortical bone at day 14. In contrast, in the diaphysis, the medullary callus gradually formed until day 14 (Fig. 3A, C). The bone aperture filled with medullary callus transiently at day 14, and then the medullary callus was rapidly resorbed at day 21. There were significant differences between the two sites at days 5, 7, 21, 35, and 42 (Fig. 3C).

3.3. Recovery of BMD at the bone aperture

In normal tibias, the BMD of the cortical bone differed between the metaphysis and the diaphysis (Fig. 4A, C). The BMD of the diaphysis was nearly 1.6 times higher than that of the metaphysis.

During the repair process, BMD was gradually restored at the bone aperture at both sites (Fig. 4B, D). At day 14, the BMD was slightly higher in the metaphysis than in the diaphysis. There was no significant difference in BMD between the two sites from day 21 to day 35. At day 42, the BMD in the diaphysis was higher BMD than that in the metaphysis (Fig. 4D). Recovery to the original value occurred earlier in the metaphysis than in the diaphysis (Fig. 4E). In the metaphysis, recovery was approximately 70% and 95% at day 14 and day 35, respectively. However, BMD was not completely restored at both sites even by day 42.

3.4. Appearance of osteogenic cells and matrix in the bone marrow

As these results suggest a difference in osteogenesis in the metaphysis and diaphysis, we next examined osteogenesis in detail in both areas via histochemical and immunohistochemical analysis. ALP (an early osteoblastic marker), osteocalcin (a marker of mature osteoblasts), and type I collagen (a major bone extracellular matrix protein) were used to compare the differentiation of osteoblasts in the two bone marrows.

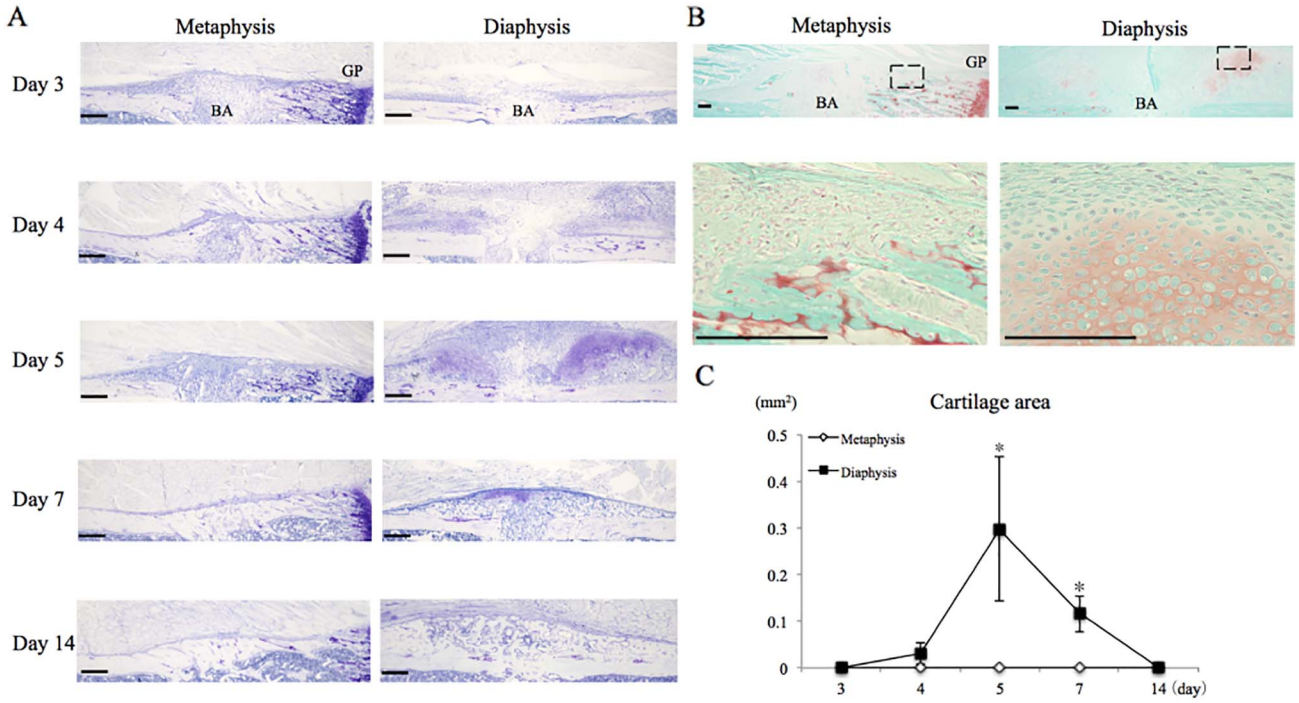

Fig. 2. Cartilage formation on the periosteum.
A. Image of periosteal region stained with toluidine blue. Bar = 200 μm.
B. Image of periosteal region stained with safranin o/fast green on day 5(top), and high magnification of square (bottom). Bar = 100 μm BA = Bone Aperture, GP = Growth Plate.
C. Quantification of metachromatic area. * = $P < 0.05$.
There was significant difference in metachromatic area between both sites at day 5 and 7.

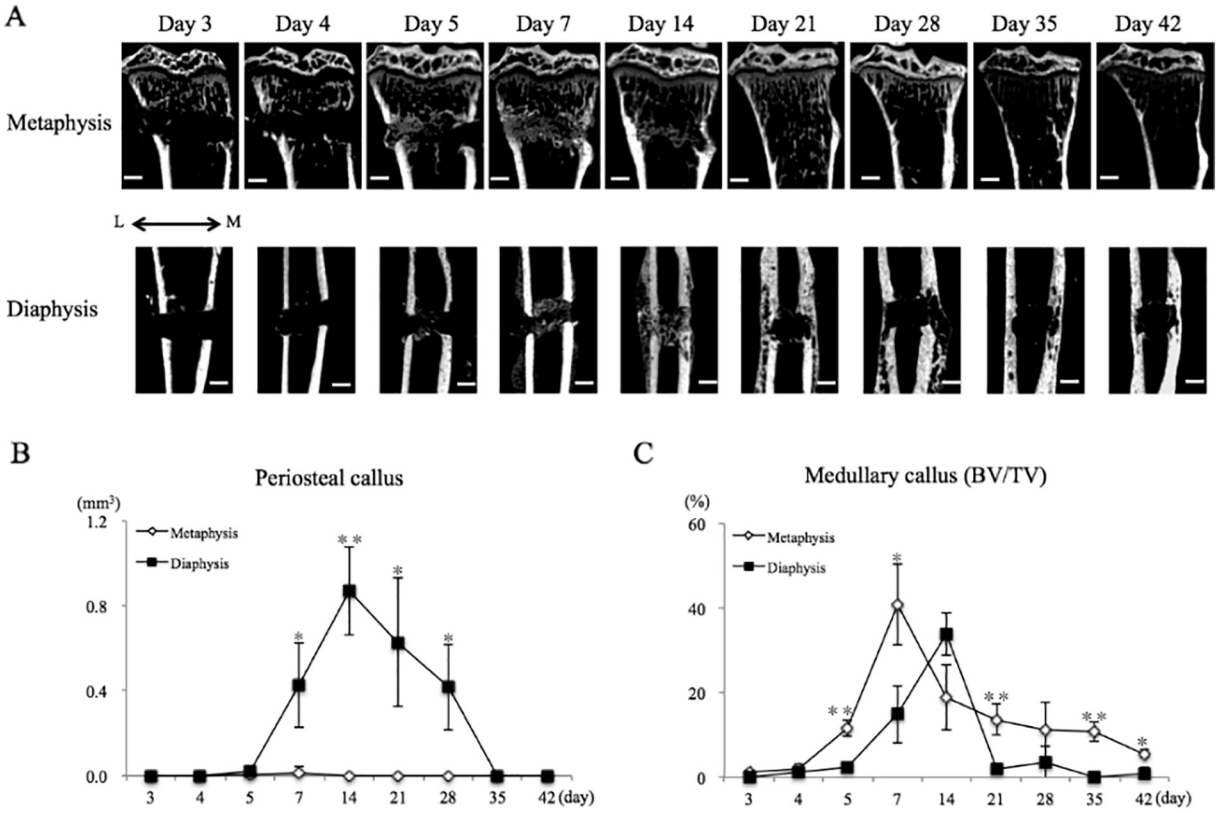

Fig. 3. Callus formation pattern is different in the two regions.
A. Representative of micro-CT images during repair process in two sites.
B. Quantification of periosteal callus formation. In the metaphysis, a small amount of bone formation was observed at days 5 and 7.
C. Quantification of medullary callus formation. Medullary callus was formed earlier in the metaphysis compared with the diaphysis. L = Lateral side, M = Medial side, Bar = 500 μm, * = $P < 0.05$, ** = $P < 0.01$.

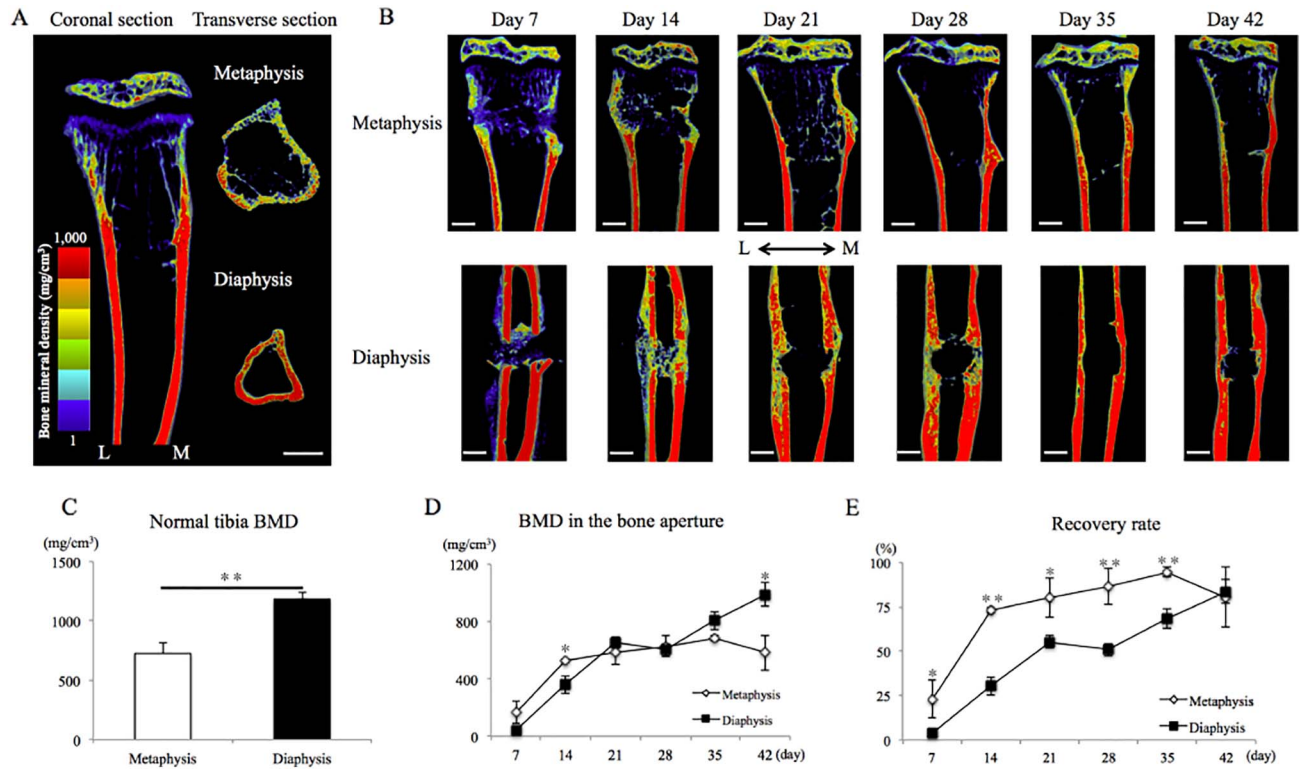

Fig. 4. BMD in the normal tibia and bone aperture.
A. Visualization of BMD in normal tibia. B. Representative of BMD during repair process in both sites.
C. BMD at the two regions in normal tibia. The diaphysis was nearly 1.6 times higher than those of the metaphysis.
D. Changes in BMD during repair process. BMD was gradually restored at bone aperture in two sites.
E. Recovery rate to original value. Metaphysis was restored earlier than diaphysis.
L = Lateral side, M = Medial side, Bar = 500 μm * = $P < 0.05$, ** = $P < 0.01$.

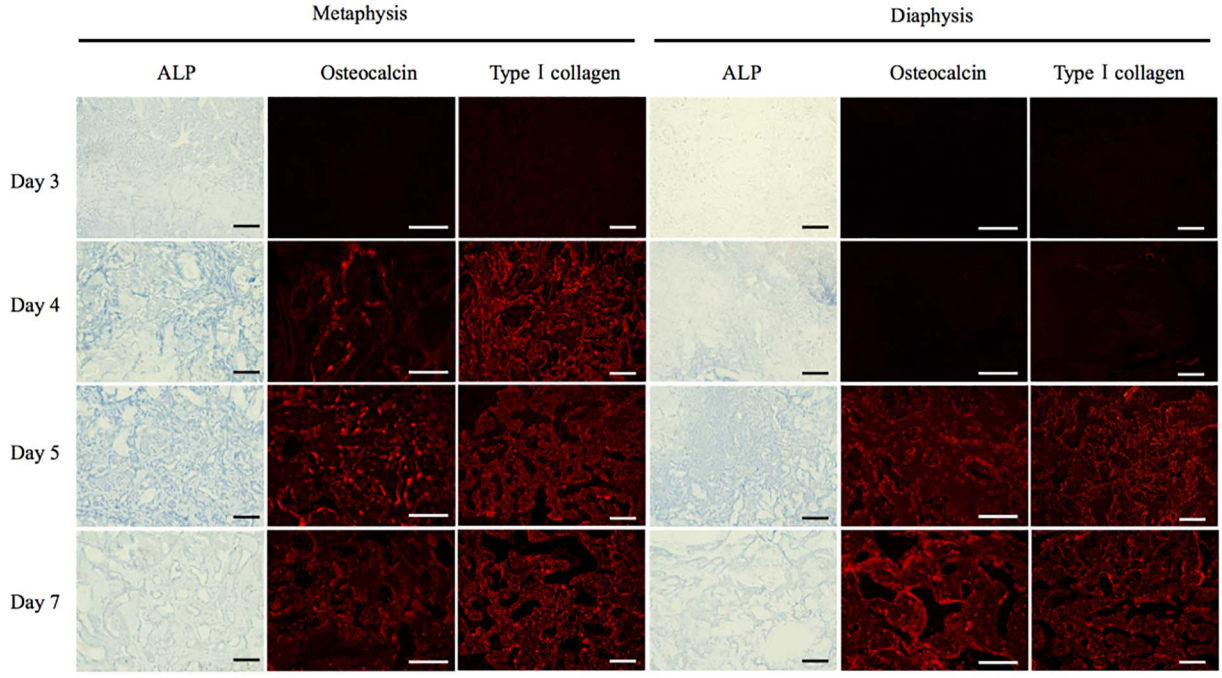

Fig. 5. Appearance of osteogenic cells and matrix in the bone marrow.
Expression of the osteogenic markers appeared earlier in the metaphysis than the diaphysis. Bar = 100 μm.

In the metaphysis, cells in the bone marrow began to express ALP activity at day 3 (Fig. 5). The activity of ALP increased up to 5 days and then decreased. In the diaphysis, ALP was not detected in bone marrow cells on day 3 (Fig. 5) but instead was detected beginning on day 4, and also showed a maximum at 5 days.

Osteocalcin was detected in the bone marrow cells of the metaphysis on day 4 (Fig. 5). From days 5 to 7, osteocalcin was widely detected in the bone marrow cells. In the case of the diaphysis,

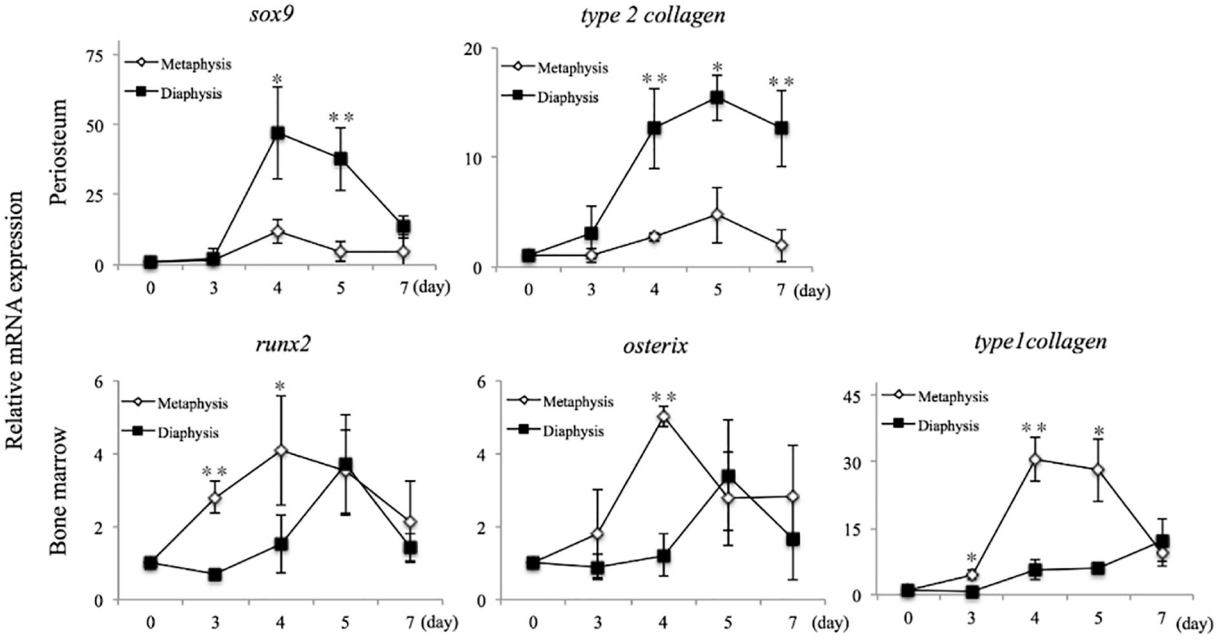

Fig. 6. The mRNA expression of chondrogenesis and osteogenesis markers.
In the diaphysis, the mRNA expression of chondrogenesis markers significantly increased compared with that of metaphysis on the periosteal side. The mRNA expression of osteogenesis markers was earlier in the metaphysis than the diaphysis in the bone marrow. * = $P < 0.05$, ** = $P < 0.01$.

osteocalcin was first detected in the bone marrow cells on day 5, and the number of cells expressing osteocalcin increased until day 7.

In the metaphysis, type I collagen was detected on day 4, but in the diaphysis, it was not detected until day 5 (Fig. 5).

3.5. mRNA expression

3.5.1. Chondrogenesis in the periosteum

To confirm the presence of chondrogenesis, we analyzed the expression of *sox9* and *type 2 collagen* mRNAs in the periosteum by qPCR. Both mRNAs were markedly upregulated in the diaphysis from day 4 compared to levels in the metaphysis (Fig. 6). In the diaphysis, the expression of *type 2 collagen* mRNA peaked on day 5 while the expression of *sox9* mRNA peaked on day 4. Significant differences in *sox9* and *type 2 collagen* expression were observed between the metaphysis and the diaphysis on days 4 and 5 and on days 4, 5, and 7, respectively.

3.5.2. Osteogenesis within the bone marrow

In the metaphysis, *runx2* and *osterix* mRNA expression was markedly upregulated on days 3 and 4 (Fig. 6). In the diaphysis, both mRNAs gradually increased from day 4 to day 5. Significant differences in *runx2* and *osterix* expression were found between the metaphysis and the diaphysis on days 3 and 4 and on day 4, respectively. The expression of *type 1 collagen* mRNA was significantly elevated on days 3 to 5 in the metaphysis, which was earlier than in the diaphysis.

4. Discussion

In this study, we clearly demonstrated differences in the bone repair processes of drill-holes placed in the metaphysis and the diaphysis. In the diaphysis, cartilage formed at the periosteal region, while little to no cartilage tissue formation was induced in the metaphysis. Furthermore, newly formed bone in the bone marrow developed on the cortical bone side and finally filled the bone aperture in the metaphysis.

It has been reported that the cartilaginous callus may arise from the periosteum (Ozaki et al., 2005; Murao et al., 2013), bone marrow (Colnot et al., 2006), and from circulating cells (Shirley et al., 2005). Among these, the periosteum is believed to play an essential role in the bone repair process, as the removal of the periosteum in a tibial fracture model results in poor callus formation (Ozaki et al., 2005). Recently, a genetic lineage tracing study revealed that periosteal cells are the major source of the cartilaginous callus during the bone repair process (Murao et al., 2013). The periosteum consists of two distinct layers, an outer fibrous layer and an inner layer that has significant osteogenic and chondrogenic potential (Bilkay et al., 2008; Ito et al., 2001).

Chondrocytes are derived from mesenchymal stem cells, and the transcription factor SOX9 is a key regulator of chondrocyte differentiation and of type II collagen gene expression (Bell et al., 1997). In the bone repair process, mesenchymal stem cells in the periosteum differentiate into chondrocytes and form the cartilaginous callus. Mesenchymal stem cells exist in various tissues and exhibit different chondrogenic potentials (Heo et al., 2016). Differences in the thickness and cell composition of the periosteum are based on age and bone region (metaphysis vs. diaphysis) (Fan et al., 2008). The ability of periosteal cells to undergo chondrogenesis differs between cells derived from the various bones (Gallay et al., 1994), and this ability decreases with age (O'Driscoll et al., 2001). In this study, chondrogenic mRNA expression was slightly upregulated by RT-PCR, however cartilage tissue was not detected in bone healing sites of the metaphysis by histological analysis. This result raises the possibility that these mRNA expression levels might be too weak for a complete chondrogenesis response or that some of unknown factors might inhibit the chondrogenesis. In any case, chondrogenic activity of mesenchymal cells in periosteum in response to the bone fracture appears to be different between in the metaphysis and diaphysis.

Cells in the bone marrow appear to be the sources of medullary callus formation, as a medullary callus is not observed when the bone marrow is ablated during the bone repair process (Amsel et al., 1964). Bone marrow cells have strong osteogenic potential, and following injury, these cells exhibit enhanced osteogenic potential (Marecic et al., 2015). Mesenchymal stem cells residing close to the bone surface show strong osteogenic potential in comparison with that of cells located in the central region of the bone marrow (Siclari et al., 2014). The bone marrow microenvironment differs between the metaphysis and the diaphysis. The metaphyseal region is rich in cancellous bone, and thus contains more abundant mesenchymal stem cells with strong osteogenic

potential than the diaphyseal region. This suggests that the metaphyseal region may be better able to recruit cells to the bone injury site, but there is not yet any clear evidence of this. The present study demonstrated that osteogenic cells and medullary callus appear earlier in the metaphysis than in the diaphysis within bone marrow. This result strongly suggests that the metaphyseal region is more conducive to the recruitment of mesenchymal stem cells to injured bone marrow than the diaphyseal region.

BMD is an important factor in bone strength (Ammann and Rizzoli, 2003). In this study, BMD was restored earlier in the metaphysis than in the diaphysis. However a bone strength test was not determined in both sites. In a drill-holes model, the strength of newly formed bone of bone strength is analyzed by pull-out test, but this analysis is limited to newly formed bone around an inserted screw (Bernhardsson et al., 2015). A bone strength test should be considered in future work to better understand bone strength recovery during these two bone repair processes.

Limitation of this study is that adolescent mice were used as experimental animals. Thus, the skeletons in these mice are not mature, and have great healing capacity compared to mice in the middle age and elderly [Lu et al., 2005]. The results of this study do not necessarily reflect what might occur in skeletally mature adult mice. Future studies should investigate whether bone healing in these two sites is different in older mice.

5. Conclusions

Our findings indicate several differences in the bone repair processes of the metaphysis and the diaphysis, suggesting functional heterogeneity of the periosteum and bone marrow mesenchymal cells in response to bone injury.

Conflicts of interest

The authors have no conflicts of interest.

Acknowledgments

The part of this study was supported by the Grant-in-Aid for Scientific Research (15K11022) from the Ministry of Education, Culture, Sports, Science and Technology of Japan. This study was also in part supported by High-Tech Research Center Project for Private Universities from Ministry of Education, Culture, Sports, Science and Technology, Japan.

References

Ammann, P., Rizzoli, R., 2003. Bone strength and its determinants. Osteoporos. Int. Suppl. S13–8. http://dx.doi.org/10.1007/s00198-002-1345-4.

Amsel, S., Maniatis, A., Tavassoli, M., Crosby, W.H., 1964. The significance of intramedullary cancellous bone formation in the repair of bone marrow tissue. Anat. Rec. 164 (1), 101–111. http://dx.doi.org/10.1002/ar.1091640107.

Aspenberg, P., Sandberg, O., 2012. Distal radial fractures heal by direct woven bone formation. Acta Orthop. 84 (3), 297–300. http://dx.doi.org/10.3109/17453674.2013.792769.

Bell, D.M., Leung, K.K., Wheatley, S.C., Ng, L.J., Zhou, S., Ling, K.W., Sham, M.H., Koopman, P., Tam, P.P., Cheah, K.S., 1997. SOX9 directly regulates the type-II collagen gene. Nat. Genet. 16 (2), 174–178. http://dx.doi.org/10.1038/ng0697-174.

Bernhardsson, M., Sandberg, O., Aspenberg, P., 2015. Experimental models for cancellous bone healing in the rat comparison of drill holes and implanted screws. Acta Orthop. 86 (6), 745–750. http://dx.doi.org/10.3109/17453674.2015.1075705.

Bilkay, U., Tokat, C., Helvaci, E., Ozek, C., Zekioglu, O., Onat, T., Songur, E., 2008. Osteogenic capacities of tibial and cranial periosteum: a biochemical and histologic study. J. Craniofac. Surg. 19 (2), 453–458. http://dx.doi.org/10.1097/SCS.0b013e318052fe3d.

Bonnarens, F., Einhorn, T.A., 1984. Production of a standard closed fracture in laboratory animal bone. J. Orthop. Res. 2 (1), 97–101. http://dx.doi.org/10.1002/jor.1100020115.

Brown, C., Heckman, D., McKee, M., McQueen, M., Ricci, W., Tornetta, P., 2014. Rockwood and Green's Fractures in Adults, 8th edition. LIPPINCOTT WILLIAMS & WILKINS, Pennsylvania.

Chen, W.T., Han da, C., Zhang, P.X., Han, N., Kou, Y.H., Yin, X.F., Jiang, B.G., 2015. A special healing pattern in stable metaphyseal fractures. Acta Orthop. 86 (2), 238–242. http://dx.doi.org/10.3109/17453674.2014.1003127.

Colnot, C., Huang, S., Helms, J., 2006. Analyzing the cellular contribution of bone marrow to fracture healing using bone marrow transplantation in mice. Biochem. Biophys. Res. Commun. 350 (3), 557–561. http://dx.doi.org/10.1016/j.bbrc.2006.09.079.

Corrales, L.A., Morched, S., Bandari, M., Miclau, T., 2008. Variability in the assessment of fracture-healing in orthopaedic trauma studies. J. Bone Joint Surg. Am. 90 (9), 1862–1868. http://dx.doi.org/10.2106/JBJS.G.01580.

Driessen, J.h.M., Hansen, L., Eriksen, S.A., Onzenoort, H.A.W., Henry, R.M.A., van den Bergh, J., brahamsen, B., Vestergaard, P., de Vries, F., 2016. The epidemiology of fractures in Denmark in 2011. Osteoporos. Int. 27 (6), 2017–2025. http://dx.doi.org/10.1007/s00198-016-3488-8.

Einhorn, T.A., Gerstenfeld, L.C., 2015. Fracture healing: mechanisms and interventions. Nat. Rev. Rheumatol. 11, 45–54. http://dx.doi.org/10.1038/nrrheum.2014.164.

Fan, W., Crawford, R., Xiao, Y., 2008. Structural and cellular differences between metaphyseal and diaphyseal periosteum in different aged rats. Bone 42 (1), 81–89. http://dx.doi.org/10.1016/j.bone.2007.08.048.

Gallay, S.H., Miura, Y. Commisso, Fitzsimmons, J.S., O'Driscoll, S.W., 1994. Relationship of donor site to chondrogenic potential of periosteum in vitro. J. Orthop. Res. 12 (4), 515–525. http://dx.doi.org/10.1002/jor.1100120408.

Guarnerio, J., Coltella, N., Ala, U., Tonon, G., Pandolfi, P.P., Bernardi, R., 2014. Bone marrow endosteal mesenchymal progenitors depend on HIF factors for maintenance and regulation of hematopoiesis. Stem Cell Rep. 2 (6), 794–809. http://dx.doi.org/10.1016/j.stemcr.2014.04.002.

Han, D., Han, N., Xue, F., Zhang, P., 2015. A novel specialized staging system for cancellous fracture healing, distinct from traditional healing pattern of diaphysis corticalfracture? Int. J. Clin. Exp. Med. 15 (8), 1301–1304.

He, Y.X., Zhang, G., Pan, X.H., Liu, Z., Zheng, L.Z., Chan, C.W., Lee, K.M., Cao, Y.P., Li, G., Wei, L., Hung, L.K., Leung, K.S., Qin, L., 2011. Impaired bone healing pattern in mice with ovariectomy-induced osteoporosis: a drill-hole defect model. Bone 48 (6), 1340–1388. http://dx.doi.org/10.1016/j.bone.2011.03.720.

Hedström, E.M., Svensson, O., Bergström, U., Michno, P., 2010. Epidemiology of fractures in children and adolescents increased incidence over the past decade: a population-based study from northern Sweden. Acta Orthop. 81 (1), 148–153. http://dx.doi.org/10.3109/17453671003628780.

Heo, J.S., Choi, Y., Kim, K.S., Kim, H.O., 2016. Comparison of molecular profiles of human mesenchymal stem cells derived from bone marrow, umbilical cord blood, placenta and adipose tissue. Int. J. Mol. Med. 37 (1), 115–125. http://dx.doi.org/10.3892/ijmm.2015.2413.

Histing, T., Garcia, P., Holstein, J.H., Klein, A.M., Matthys, A.R., Nuetzi, R., Steck, R., Laschke, M.W., Wehner, T., Bindl, R., Recknagel, S., Stuermer, E.K., Vollmar, B., Wildemann, B., Lienau, J., Willie, B., Peters, A., Ignatius, A., Pohlemann, T., Claes, L., Menger, M.D., 2011. Small animal bone healing models: standards, tips, and pitfalls results of a consensus meeting. Bone 49 (4), 591–599. http://dx.doi.org/10.1016/j.bone.2011.07.007.

Ito, Y., Fitzsimmons, J.S., Sanyal, A., Mello, M.A., Mukherjee, N., O'Driscoll, S.W., 2001. Localization of chondrocyte precursors in periosteum. Osteoarthr. Cartil. 9 (3), 215–223. http://dx.doi.org/10.1053/joca.2000.0378.

Jarry, J., Uhthoff, H., 1971. Differences in healing of metaphyseal and diaphyseal fractures. Can. J. Surg. 14, 127–135.

Lu, C., Miclau, T., Hu, D., Hansen, E., Tsui, K., Puttlitz, C., Marcucio, R.S., 2005. Cellular basis for age-related changes in fracture repair. J. Orthop. Res. 23 (6), 1300–1307. http://dx.doi.org/10.1016/j.orthres.2005.04.003.1100230610.

Marecic, O., Tevlin, R., McArdle, A., Seo, E.Y., Wearda, T., Duldulao, C., Walmsley, A., Nguyen, G.G., Weissman, I.L., Chan, C.K.F., Longaker, M.T., 2015. Identification and characterization of an injury-induced skeletal progenitor. Proc. Natl. Acad. Sci. U. S. A. 112 (32), 9920–9925. http://dx.doi.org/10.1073/pnas.1513066112.

Mills, L.A., Simpson, A.H., 2012. In vivo models of bone repair. J. Bone Joint Surg. (Br.) 94 (7), 865–874. http://dx.doi.org/10.1302/0301-620X.94B7.27370.

Murao, H., Yamamoto, K., Matsuda, S., Akiyama, H., 2013. Periosteal cells are a major source of soft callus in bone fracture. J. Bone Miner. Metab. 31 (4), 390–398. http://dx.doi.org/10.1007/s00774-013-0429-x.

O'Driscoll, S.W., Saris, D.B., Ito, Y., Fitzimmons, J.S., 2001. The chondrogenic potential of periosteum decreases with age. J. Orthop. Res. 19 (1), 95–103. http://dx.doi.org/10.1016/S0736-0266(00)00014-0.

Ozaki, A., Tsunoda, M., Kinoshita, S., Saura, R., 2005. Role of fracture hematoma and periosteum during fracture healing in rats: interaction of fracture hematoma and the periosteum in the initial step of the healing process. J. Orthop. Sci. 5 (1), 64–70. http://dx.doi.org/10.1007/s007760050010.

Postacchini, F., Gumina, S., Perugia, D., Martino, C., 1995. Early fracture callus in the diaphysis of human long bones. Histologic and ultrastructural study. Clin. Orthop. Relat. Res. (310), 218–228.

Sandberg, O., Aspenberg, P., 2015a. Different effects of indomethacin on healing of shaft and metaphyseal fractures. Acta Orthop. 86 (2), 243–247. http://dx.doi.org/10.3109/17453674.2014.973328.

Sandberg, O., Aspenberg, P., 2015b. Glucocorticoids inhibit shaft fracture healing but not metaphyseal bone regeneration under stable mechanical conditions. Bone Joint. Res. 4 (10), 170–175. http://dx.doi.org/10.1302/2046-3758.410.2000414.

Sandberg, O., Bernhardsson, M., Aspenberg, P., 2016. Earlier effect of alendronate in mouse metaphyseal versus diaphyseal bone healing. J. Orthop. Res. 35 (4), 793–799. http://dx.doi.org/10.1002/jor.23316.

Schindeler, A., McDonald, M.M., Bokko, P., Little, D.G., 2008. Bone remodeling during fracture repair: the cellular picture. Semin. Cell Dev. Biol. 19 (5), 459–466. http://dx.doi.org/10.1016/j.semcdb.2008.07.004.

Shirley, D., Marsh, D., Jordan, G., McQuaid, S., Li, G., 2005. Systemic recruitment of osteoblastic cells in fracture healing. J. Orthop. Res. 23 (5), 1013–1021. http://dx.doi.org/10.1016/j.orthres.2005.01.013.
Siclari, V.A., Zhu, J., Akiyama, K., Liu, F., Zhang, X., Chandra, A., Nah, H.D., Shi, S., Qin, L., 2014. Mesenchymal progenitors residing close to the bone surface are functionally distinct from those in the central bone marrow. Bone 53 (2), 575–586. http://dx.doi.org/10.1016/j.bone.2012.12.013.
Standring, S., 2015. Gray's Anatomy, 41th edition. Churchill Livingstone, London.
Uhthoff, H., Rahn, B.A., 1981. Healing patterns of metaphyseal fracture. Clin. Orthop. Relat. Res. 160, 295–303.